Reduced Projection Algorithm for 2D Cephalograms Derived from 3D CBCT Images in Orthodontics

BY

ABDELRAHMAN SALEM
D.D.S., University of Jordan, Amman, Jordan 2009

THESIS

Submitted as partial fulfillment of the requirements
For the degree of Master of Science in Oral Sciences
In the Graduate College of the
University of Illinois at Chicago, 2014
Chicago, Illinois

Defense Committee:

Budi Kusnoto, Advisor
Carla A. Evans
Robert Manasse
Grace Viana, MSc
Xiaochuan Pan, University of Chicago

ACKNOWLEDGEMENTS

I would like to thank my thesis committee, Dr. Budi Kusnoto, Dr. Carla Evans, Dr. Xiaochuan Pan, Dr. Robert Manasse and Mrs. Grace Viana for their influential support and assistance throughout this process.

AIS

TABLE OF CONTENTS

LIST OF TABLES

LIST OF FIGURES

LIST OF ABBREVIATIONS

2D	Two Dimensional
3D	Three Dimensional
ASD-POCS	adaptive-steepest-descent-projection-onto-convex-sets algorithm
CBCT	Cone Beam Computed Tomography
CT	Computed Tomography
DICOM	Digital Imaging and Communications in Medicine (DICOM) (National Electric Manufacturers Association, Rosslyn, VA)
Dist.	Distance
FDK	Feldkamp--Davis--Kress algorithm
FOV	Field of View
Gy	Gray
iCAT	Computer assembled tomography imaging
IRB	Institutional Review Board
kVP	Kilovolt Peak
mAs	milliampere seconds
PA	Posteroanterior
SNR	Signal to Noise Ratio
Sv	Sievert
UC	University of Chicago

SUMMARY

Cone Beam Computed Tomography (CBCT) has become an increasingly important tool in treatment planning and diagnosis in orthodontics. The popularity of CBCT has increased tremendously among dentists and orthodontists. Unfortunately, the increase in the ionizing radiation and reports in the lay press about radiation overdose with CT scanners created arguments against CBCT as the imaging technique of choice for comprehensive orthodontic assessment.

The purpose of this feasibility study is to find a threshold number of projections produced by the Adaptive-Steepest-Descent-Projection-Onto-Convex-Sets (ASD-POCS) algorithm from the original iCAT 3D CBCT to be used reliably for 2D evaluation of orthodontic diagnostic records.

Virtual 3D digital images of craniofacial structures were made by the iCAT CBCT machine (Imaging Sciences International, Hatfield, Pa) of four subjects. The ASD-POCS algorithm was used to derive different compression rates by reconstructing the 3D digital images using lower number of projections. Five different compression rates were compared (320iCAT, 300 UC, 151 UC, 76 UC, and 39 UC). Dolphin 3D (Version 11.7, Dolphin Imaging, Chartsworth, CA) was used to project the 3D images of different compression rates into lateral and postero-anterior (PA) cephalograms. The accuracy of landmark identification in cepahlograms derived from different compression rates was used to evaluate the quality of compressions.

The preliminary results of this feasibility study based on the small sample (n=4), showed that there is no mean difference of error distances between a set of landmark locations in both

lateral and PA cephalometric radiographs derived from CBCT images at different compression rates. None of the means of error distances of landmark locations in different compressions rates exceeded 1.5 mm error margin for both lateral and PA cephalometric radiographs.

1. INTRODUCTION

1.1. Backgroud

CBCT in Orthodontics:

Cone beam computed tomography (CBCT) is a three dimensional imaging technique used in dentistry and medicine. CBCT has become an increasingly important tool in treatment planning and diagnosis in implant dentistry, and more recently in other dental fields including endodontics and orthodontics. The popularity of CBCT has grown tremendously among dentists and orthodontists, perhaps because of increased access to such technology.

“During a CBCT scan, the scanner rotates around the patient's head, obtaining up to nearly 600 distinct images. The scanning software collects the data and reconstructs it, producing what is termed a digital volume composed of three dimensional voxels of anatomical data that can then be manipulated and visualized with specialized software” (Hatcher et al, 2010).

The benefits of CBCT in orthodontics include: the accuracy of image geometry and measurements by eliminating the image magnification and distortion commonly encountered in 2D radiographs. Potential uses of CBCT are precise localization of ectopic teeth and precise measurement of unerupted tooth sizes, assessment of root resorption, identification and quantification of asymmetry, visualization of airway abnormalities, assessment of periodontal structures, identification of endodontic problems, viewing condylar positions and

temporomandibular joint bony structures, determination of placement sites for temporary skeletal anchorage devices, measurement of bone density, visualizing root proximity and resorption, and even providing the imaging data to support treatment simulation and technology-aided treatment (Larson, 2012)

Unfortunately, the increased ionizing radiation exposure created an argument against CBCT as the imaging technique of choice for comprehensive orthodontic assessment and resulted in the development of general guidelines to deal with justification, optimization and referral criteria for users of dental CBCT. Such guidelines were adopted by the American Association of Orthodontists in 2010: “the AAO recognizes that while there may be clinical situations where a cone-beam computed tomography (CBCT) radiograph may be of value, the use of such technology is not routinely required for orthodontic radiography”. The American Academy of Oral and Maxillofacial Radiology (AAOMR) developed this position statement “the use of CBCT in orthodontic treatment should be justified on an individual basis, based on clinical presentation. This statement provides general recommendations, specific use selection recommendations, optimization protocols, and radiation-dose, risk-assessment strategies for CBCT imaging in orthodontic diagnosis, treatment and outcomes”.

Construction of 3D imaging

The 3D imaging of the maxillofacial region is composed of a series of 2-D digital images. A pixel is the basic unit of a 2D image and it is represented by height and width. A voxel has a height, width, and depth. Medical CT is one of the first 3D radiographic imaging techniques used in the field of medicine. “A typical voxel size of a medical CT scan of the maxillofacial complex is [vx, vy, vz] = [0.4 mm, 0.4 mm, 1 mm]” (Gwen et al, 2005). When all these CT slices are combined, a block of a 3D volume is obtained (Fig. 1).

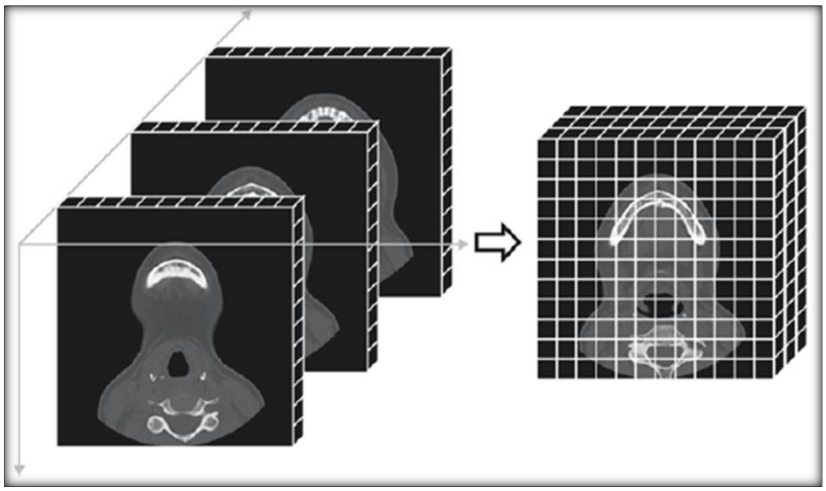

Figure 1. Combining 2D slices into 3D volume

After passing through the craniofacial tissues, the X-ray beams are received by special detectors. Algorithms are used by the machine to reconstruct the images captured digitally. The 3D volume consists of voxels, the basic unit of a 3D image. These voxels are represented digitally and can be stored and sent electronically.

To visualize how these 3D volumes can be represented with numbers, it is very important to understand how the 3D image is constructed. When the CT numbers at the intersection between different 2D slices are calculated, a 3D image can be constructed and re-

sliced in a different plane (Fig. 2). Various cuts in the volume can be measured and reconstructed (Gwen et al, 2005).

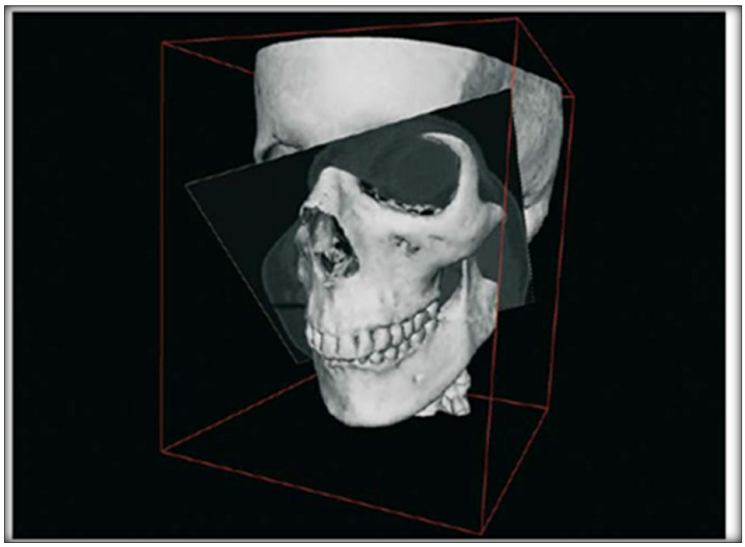

Figure 2. Computing CT numbers and re-slicing

The X-ray beam is generated by the X-ray tube and penetrates through the tissues of the maxillofacial complex. These x-rays produce a radiograph with a specific resolution(Fig. 3). The resolution is related to the quality of the anode tip used in the x-ray machine, the size of the patient (dense bone increases X-ray scattering causing deterioration) and the way these x-rays are converted to a 2D radiograph (Gwen et al, 2005).

Each CT number is associated with an opacity value that represents the opacity of specific craniofacial tissues encountered by the beam. This results in a final grey value on the image. The contrast of these projections can be adjusted by modifying the window/level settings in the CT machine (Gwen et al, 2005).

Each 2D slice obtained has a specific dose. Therefore, the higher number of 2D slices used to construct the 3D image, the higher radiation is expected. In order to reduce the radiation dose, a smaller number of 2D slices can be used. However, a less accurate image with more noise and irregularities will be obtained due to this lower dose (Gwen et al, 2005).

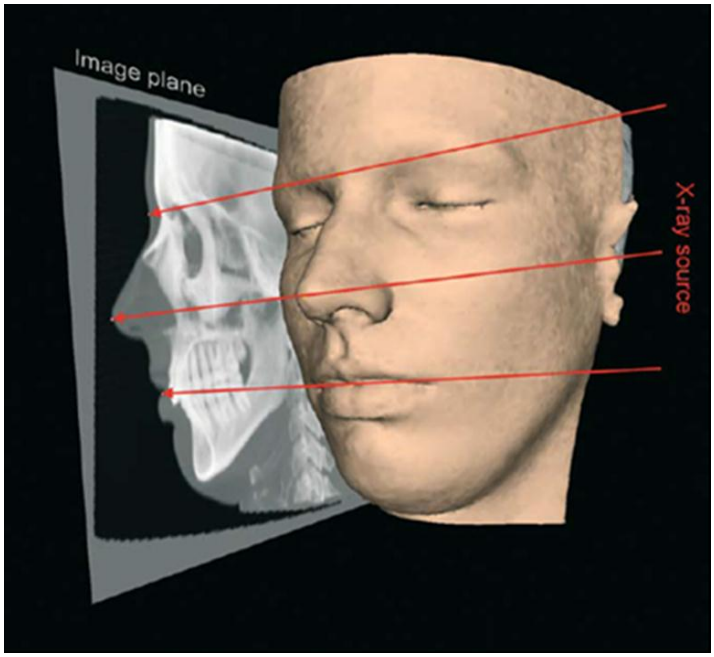

Figure 3. Lateral cephalogram computed from 3D volume

1.2. Specific Aims

The purpose of this feasibility study is to find a threshold number of projections derived by the ASD-POCS algorithm from the original iCAT 3D CBCT data set which still produces accurate cephalometric landmarks locations based on 2D lateral and PA cephalograms as part of orthodontic diagnostic imaging.

2. REVIEW OF LITERATURE

2.1 CBCT in Dentistry and Radiation

The technologic advancements of the last thirty years have changed the practice of dentistry immensely. With every new technology that comes forward, a period of inquisitive discovery is necessary to determine a standard of care. Three dimensional (3D) radiographic technologies are a recent diagnostic tool to become available to the healing arts. CBCT machines that replaced high dose, large data loaded medical Computed Tomography scans (CTs) have brought dentistry in the world of 3D imaging. With the introduction of the new low cost and low dose CBCT machines, interest in using CBCT for an increasing number of dental procedures has increased dramatically.

This technology can be used by orthodontists to obtain accurate information that helps them in the process of diagnosis and treatment planning. However, because children and adolescents are particularly vulnerable to radiation, many experts in dental radiation have raised alarms about putting patients at risk, particularly younger patients (Walt and Jo, 2010).

Various tissues in the body react to ionizing radiation in different ways. Initially, radiation risk was determined by data from outdated therapeutic techniques that later resulted in cancers. Ionizing radiation “hit” the cell nucleus and disrupt mitosis and or damage DNA. These mutations are random and may or may not increase one’s risk for cancer. If a cell is rapidly dividing, there is a greater chance that the mutation will pass on to later cellular

generations. The various tissues are weighted by their sensitivity to radiation as well as the actual dose they receive from the radiograph (Brooks, 2009).

Ludlow and co-workers (2008) describes the effective dose as the dose quantity related to probability of health detriment due to effects of exposure to low doses of ionizing radiation. This information allows for a more accurate description of the radiation dose subjected to the patient with various imaging technologies and different imaging techniques and safety precautions.

The International Commission on Radiological Protection (ICRP) revised their 1990 recommendations in 2007 to reflect new tissue data. New information from studies in Japan on cancer incidence and mortality data in Japanese patient exposure to the atomic bomb in Hiroshima and Nagasaki caused the ICRP to reevaluate the effect of radiation on salivary glands, thyroid glands and oral mucosa. These organs were originally listed under the broad category of remainder organs. By including these organs in effective dose calculation for dental radiographs, the effective dose increased 32-42%. When considering dental CBCTs, mandibular bone marrow, cervical spine bone marrow and salivary glands receive the highest effective dose (Tsiklakis 2006; Ludlow 2008). Although the relative risk for fatal cancers is still low, the risk is higher than previously thought (Ludlow, 2008). Much is still unknown about the exact risk for various patients and the later development of cancers, particularly in children (Brooks, 2009). It is the doctor's responsibility to weigh the diagnostic benefit with the radiation risk.

Not all CBCT machines or techniques are manufactured or used in the same way. Higher kVP and mA values increase image quality but in exchange for higher radiation dose (Brooks,

2009). Also, these modifications increase the signal to noise ratio (SNR) but not necessarily the diagnostic potential (Brooks, 2009). A study that looked at conventional CT scans used for dentistry found that reducing the dose by nine fold did not compromise diagnostic quality. Different machines have various beam and dose settings that can greatly alter the effective dose to the patients (Ludlow, 2008). It is imperative that the dentist know the CBCT settings and reduce the dose to the lowest level possible.

Tsiklakis et al (2006) compared CBCT dosimetry with and without a thyroid shield. Although the thyroid gland is not directly irradiated via the primary beam, it is affected via scatter. The thyroid has a fairly high tissue weight due to its sensitivity to ionizing radiation. By using the thyroid shield, the group was able to reduce the effective does by close to 20% without compromising image quality.

Different dental specialists and general dentists require 3D imaging for a variety of purposes. The Field of View (FOV) required for all of these procedures is not the same. An endodontist looking a specific tooth does not require the same FOV as an orthodontist interested in the entire craniofacial complex. If the diagnostic interest of the 3D image is limited to an impacted tooth perhaps a smaller FOV would serve the purpose. Obviously, the FOV reduces the amount of tissue exposed (Brooks, 2009). However, if multiple scans or images are necessary to supplement the smaller FOV, the radiation exposure is comparative, if not greater than the larger FOV, with potentially less diagnostic benefit. The 3D imaging should be tailored to fit not only the patient but the nature of the procedure.

CBCT scans allow you to see bony structures in 3D as well as traditional 2D images. A scan eliminates the need for additional cephalometric and panoramic radiographs. Tsiklakis et al (2006) found that CBCT carried 3-7 times more radiation exposure than a panoramic radiograph. One CBCT causes more radiation exposure than combined panoramic and cephalometric radiographs, thus causing more risk (Tsiklakis, 2006 and Brooks, 2009). CBCT cannot replace the need for bitewings and anterior periapical radiographs for caries detection (Brooks, 2009).

Several studies looked at the Effective Dose of CBCT in dentistry. Several studies looked at the i-CAT CBCT scanner and their use in clinical practice. CBCT exposes patient to a lower radiation dose in comparison to the conventional medical CT but still higher than the 2D images taken routinely in most dental practices (Ludlow, 2003 and 2006). Robert et al (2009) used a phantom containing thermoluminescent dosimeters for radiation dose measurements. When comparing the dosages, he found similar results to those obtained from Ludlow studies.

Ludlow et al (2008) conducted a study to compare dental CBCT and medical CT and concluded that “dental CBCT can be recommended as a dose-sparing technique in comparison with alternative medical CT scans for common oral and maxillofacial radiographic imaging tasks”.

Presently, 3D technology is simply another tool available for diagnosis and treatment planning. It can provide crucial knowledge for better treatment, but is not without risk. The health provider should view presenting CBCTs as they do prescribing a drug. They must

consider the patient as a whole, his/her age, the procedure, dose, FOV (Field of View), and cost-benefit ratio.

2.2 Iterative Reconstruction Algorithms

To have repetitive, step by step calculations, different CBCT algorithms were developed to reconstruct 3D images from a significantly reduced number of 2D projections in an effort to minimize the radiation dose required to obtain an accurate CBCT image (Emil et al, 2010). Reducing the number of projection data makes the process of image reconstruction harder because a significant part of the image is not directly captured and need to be predicted by the software. This can lead to lower quality images and more artifacts (Emil et al, 2010).

In an effort to reduce the radiation dose of medical CT, Filtered back-projection (FBP) algorithm was used for image reconstruction. Unfortunately, this algorithm showed degradation of image quality when applied to the CBCT. The FDK algorithm was also used to reduce the x-ray tube load milli-amperage (mAs). Using this algorithm produces a noisy reconstructed projection in the constructed CBCT image. To solve this problem, some techniques were used to improve these artifacts including the Algebraic reconstruction technique (ART) (Scarfe and Farman, 2008). Other algorithms used with good quality reconstructions include; CS, CS-WLS and POCS (Choi et al., 2010).

Han et al (2011) used a new algorithm to reconstruct images of medical specimens from reduced projection data and therefore, lower radiation. This new algorithm is called “the adaptive-steepest-descent-projection-onto-convex-sets (ASD-POCS) algorithm”. To validate and

evaluate the performance of the ASD-POCS algorithm, they compared different algorithms including FDK (Feldkamp--Davis--Kress algorithm) and POCS (Projection Onto Convex Sets) with the ASD-POCS. “The results showed that the ASD-POCS algorithm can yield images with a quality comparable to that obtained with existing algorithms, while using one-sixth to one quarter of the 361-view data currently used in typical micro-CT specimen imaging”.

In conclusion, micro CT studies and iterative reconstruction algorithms using parallel computing have the potential to reduce the number of projections needed to construct 3D images thus significantly reducing the amount of radiation exposure. Currently 250 minimal 2D projections are required to do full 3D reconstruction of the craniofacial region using a CBCT machine.

2.3 Comparison between 2D and 3D cephalometry

Two dimensional cephalometry has been used routinely and extensively in the diagnosis of craniofacial anomalies, orthodontics, growth monitoring and treatment progress evaluation for many years. With the rapidly increasing popularity of the 3D technology, many orthodontists started using the 3D images to obtain better representation of the craniofacial structures and deformities that cannot be detected with the regular 2D images. This presented another question, whether a 3D tracing can be used for longitudinal research in cases where there are only 2D records available.

Van Vlijmen et al (2009) conducted a study to compare 2D and 3D cephalometry on CBCT scans using 40 dry skulls. He used CBCT images to determine whether there are any

significant differences between measurements obtained from 2D radiographs and those obtained from 3D CBCT images. Seventeen landmarks were used on both the conventional 2D and the 3D images. He found that measurements obtained from 2D images were more reproducible in comparison to those obtained from 3D CBCT. He also concluded that it is not feasible to use 3D measurements in longitudinal studies where only 2D images are available from previous records.

Van Vlijmen et al (2009) also compared 2D frontal radiographs with frontal radiographs derived from CBCT. A significant difference was found between measurements made on the two different groups. Also, the measurements made on frontal radiographs obtained from the CBCT found to be more reproducible than those of the 2D radiographs.

One advantage of CBCT is the accuracy of the linear measurements regardless of the position of the patient's head. Hassan et al (2009) used CBCT scans of 8 dry skulls to evaluate the effect of rotation on the accuracy of measurements. He scanned the skulls in an ideal position first then he rotated the skulls and scanned them again. He found that small rotations do not affect the measurements significantly.

Vandenberghe et al (2009) used a sample of two skulls and evaluated thirty periodontal bone defects using intraoral 2D digital radiography and 3D CBCT. For the CBCT scans, he used the extended height mode: 129 kVp, 47.74 mA, and 40 seconds, with a resolution of 0.4 voxel. He found that measurements were comparable using both methods of imaging. He also found that the morphology of the bony defect can be more accurately described with the CBCT images but more bone details are evident on the 2D digital radiographs.

2.4 Radiation Dose and Dosimetry

"Radiation dosimetry is the measurement and calculation of the radiation dose received by matter and tissue resulting from the exposure to indirect and direct ionizing radiation. Dosimetry is focused on the calculation and analysis of internal and external dose. Internal dose is calculated from a variety of physiological techniques, while external dose is measured with a dosimeter or inferred from other radiation instruments. Medical dosimetry is the calculation of absorbed dose and optimization of dose delivery in radiation therapy. It is often performed by a professional medical dosimetrist with specialized training in the field" (International Commission on Radiation Units and Measurements (ICRU, 2011).

Radiation risk is a major concern for the growing orthodontic patients. CBCT exposes children to higher radiation dose when compared to other conventional radiographs (Grünheid et al, 2012). The ASD-POCS algorithm used in medical specimen imaging has the potential to reduce the radiation dose by reducing the number of projections needed to reconstruct the 3D CBCT image. This project uses this technology and attempts to apply it in the field of orthodontics. This project aims to evaluate the accuracy of different images constructed with the ASD-POCS algorithm for cephalometric tracing. If only a 2D lateral cephalogram is needed, the radiation from a CBCT must not be greater than the conventional 2D cephalogram.

2.5 Accuracy of cephalometric measurements.

It is important to locate the cephalometric landmarks accurately before starting with the measurements needed for orthodontic diagnosis and treatment planning of patients. Errors in

locating these landmarks can result in errors in the diagnosis and treatment plan. Baumrind and Frantz (1971) defined these errors and classified them into two major types of errors in the estimation of cranial dimensions from cephalometric radiographs. Baumrind and Frantz call the first type errors of projection. The second type they call errors of identification, which are more related to the examiner experience, the nature of the landmark and the type of cephalometric analysis used.

Baumrind and Frantz (1971) designed a study to check operator reproducibility in the identification of standard cephalometric landmarks. He asked five first year orthodontic residents to trace 20 lateral cephalometric radiographs yielding 100 tracings. The tracings were superimposed on Sella-Nasion line and an arbitrary X axis and Y axis were made. The purpose was to evaluate the accuracy of landmark identification.

Baumrind and Frantz (1971) made a graph showing the distribution of the different landmarks on an arbitrary X and Y axes. They found that specific landmarks perform in specific patterns of error. They suggested that using automatic methods, when available, can reduce these errors with the help of replicated estimates for each landmark.

In this project, Baumrind's method of locating and registering the landmarks was used to quantify the errors resulting from different compression rates and therefore, different qualities of lateral and cephalometric radiographs.

2.6 Methods of reducing the radiation dose.

Different CBCT machines produce different radiation doses. Changing the exposure settings in these machines can significantly reduce these radiation doses while maintaining the image quality at acceptable clinical level. These include: X-ray tube voltage and mAs, field of view and collimation, filtration, digital detectors, voxel size, number of projections and shielding devices.

The kilovoltage (kVp) of an X ray tube represents the energy of the x-ray beams as they move between the anode and cathode. Lower voltages results in lower energy levels and therefore less ability of the x-ray beams to penetrate into deeper tissues. This lower energy results in higher radiation of the superficial tissues such as skin (Horner, 1994). Conversely, increasing the kVp decreases exposure of the skin (Geijer et al, 2009). However, increasing the kVp also increases the scatter of the x rays beams.

Changing the tube current measured in milliamperes (mA) and the exposure time, results in a change in the number of photons emitted by the X-ray tube. Tube current and exposure time do not affect the energy of the x ray beam. Therefore, increasing mAs increases the radiation dose. However, the changing the mAs doesn't affect the penetration ability or the contrast of the radiograph. Many CBCT machines allow changing the kVp and mAs values.

The optimization of radiation dose can be defined as the process of balancing radiation dose and the image quality needed for a particular clinical procedure. Some diagnostic procedures need higher quality images and therefore higher radiation dose than others. There

is a lack of studies that attempt to optimize these two exposure factors for different CBCT units and clinical protocols. Kwong et al (2008) found that accurate detailed images can be obtained with reduced mA and kVp values. Sur et al (2010) found that the current of the x-ray beams can be significantly reduced while maintaining the quality needed for proper evaluation and planning prior to placement of dental implants.

Another method of reducing the radiation dose is to control the Field of View (FOV). Several CBCT machines employ the process of beam collimation to limit the image to the area of interest without radiating surrounding tissues unnecessarily. Smaller FOV exposes patients to lower radiation dose in comparison to larger FOV (Pauwels et al, in press).

A third method is the filtration of x ray beams. Filtration aims to remove low energy photons and reduce the radiation dose of the skin but this also might reduce the contrast of the image (Ludlow et al, 2006). Kwong et al (2008) found that the quality of the CBCT scans are not significantly affected by using these filters. Ludlow (2011) showed that a significant reduction in radiation dose can be achieved by controlling both kVp and filtration.

Using digital detectors is a fourth method to reduce the radiation dose. Two types of digital detectors are available for CBCT machines: conventional image intensifiers (II) and flat panel detectors (FPDs). FPDs have the ability to reduce the radiation dose necessary for capturing images because they are more sensitive to the photons compared with the II detectors but they are more expensive (Kalender and Kyriakou, 2007).

A fifth method is to control the voxel size. Using smaller voxel sizes results in a better resolution and quality. Unfortunately, reducing the voxel size requires increasing the radiation dose needed to capture the fine details of the exposed object (Qu et al, 2010). “The voxel size in CBCT systems may vary from less than 0.1 mm to over 0.4 mm” (Hashimoto et al, 2003; Loubele et al, 2008; Liedke et al, 2009). Again, different dental diagnostic procedures require different minimum image qualities. For example, Even though 1.25 mm voxel size is considered a highly detailed protocol for most orthodontic uses, this voxel size is not small enough to capture the thin buccal cortex of bone covering the roots of some teeth (Patcas et al, 2012).

The sixth method to reduce the radiation dose is to control the number of projections used to construct the 3D image. By increasing the number of 2D projections used to construct the 3D image, a higher quality scan with higher contrast can be obtained. However, increasing the number of 2D projections increases the radiation dose absorbed by the patient. Depending on the clinical situation, a very high resolution might not be required for that particular diagnostic task. For example, the accuracy of linear measurements are not significantly affected by changing the number of projections (Brown et al, 2009). Partial rotation has been shown to reduce the radiation dose to the patient by reducing the number of projections. Instead of the routine 360 rotation of the x-ray beam, partial rotation means that the rotation can be reduced to 180 degrees for example. This has been done successfully without significant changes on the quality of the images (Lofthag-Hansen et al, 2010).

Using lead shielding devices significantly reduced the radiation dose to the thyroid gland during the CBCT exposure (Tsiklakis et al, 2005). Shielding devices have been used for a long time for the conventional 2D radiography and they are still used now.

A number of different ways of reducing the radiation dose have been evaluated. This project aims, with the use of ASD-POCS algorithm, to assess further the effect of the number of projections on image quality and radiation dose

3. METHODOLOGY

3.1 Sample

The experimental sample in this feasibility study consisted of 4 CBCT scans of patients from the Department of Orthodontics .The CBCT scans were selected from a larger sample according to the following criteria: (1) fully developed permanent dentition (2) normal skull morphology (3) all images have to be of high quality (4) central incisors and first molars must be present (5) a reproducible, stable occlusion. Exclusion criteria factors were those that will create confusion for landmark identification: (1) craniofacial deformities including clefts and abnormal jaw morphology (2) presence of deciduous teeth.

3.2 IRB Approval

A "Determination of Whether an Activity Represents Human Subjects Research" application was submitted to the UIC Office for the Protection of Research Subjects. The UIC OPRS determined on 12/3/13 that my study did not meet the definition of human subject research and therefore this study was exempt and did not require further submission to the IRB. Protocol number: IRB # 2013-1120

3.3 Methods and Materials

Four CBCT scans were taken from Department of Orthodontics archives at the University of Illinois at Chicago with calibrated position at the maximum (100%) amount of radiation producing the highest quality image. The Frankfort Horizontal plane was used as parallel as possible to the floor to determine the orientation of the CBCT images.

The CBCT scans were taken for the 4 patients with the i-CAT Next Generation scanner (Imaging Sciences International, Hatfield, PA, USA) using a 0.3 voxel size scan with diameter of 16 cm and height of 13 cm yielding 5 mAs and 120 kVp to be cited as the full 100% radiation scan.

The original Digital Imaging and Communications in Medicine (DICOM) files of the 4 patients were de-identified online using trial wire website. The ASD-POCS algorithm was used to reduce the number of projections via compressed 3D CT iterative reconstruction which simulates various compression rates. The original iCAT image is composed of 320 projections. These projections were reduced using the ASD-POCS algorithm. New 3D images were reconstructed using fewer projections. The algorithm was used to construct the 3D images with 300, 151, 76, 39 projections resulting in 5 different compression rates (320iCAT, 300 UC, 151 UC, 76 UC, 39 UC) Figure 4.

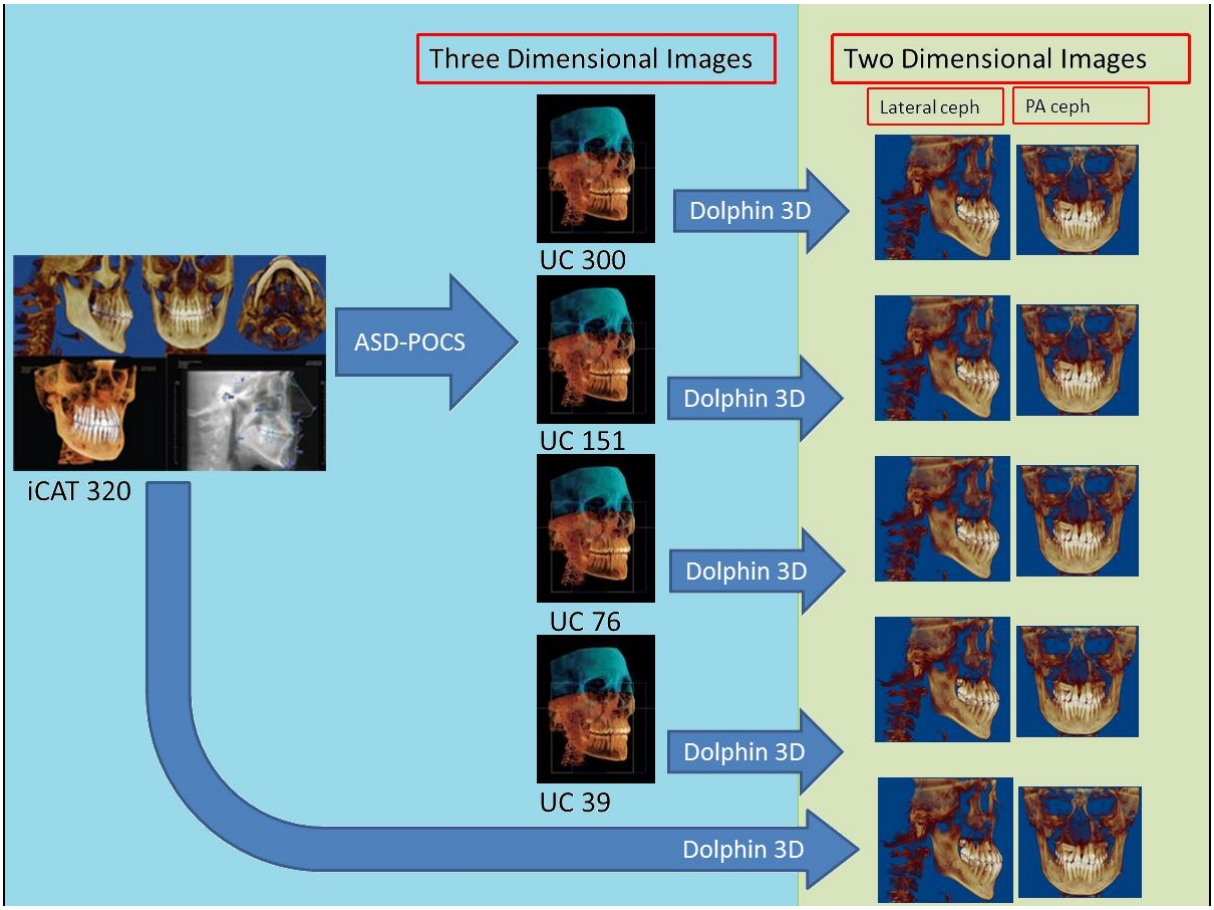

Figure 4. Obtaining compressions and 2D cephalograms.

Raw data was stored in DICOM format. The CBCT data was imported into Dolphin 3D software (Version 11.7, Dolphin Imaging, Chartsworth, CA). Five different CBCT images for each subject were projected into a lateral and PA (postero-anterior) cephalometric radiographs (using anatomical midsagittal plane). Dolphin 3D (Version 11.7, Dolphin Imaging, Chartsworth, CA) was used to project the 3D images into 2D lateral and PA cephalometric images. The standard lateral and PA (postero-anterior) cephalometric landmarks were then analyzed for accuracy of landmark identification by the investigators with a mean error of < 1.5 mm.

A grid with a horizontal x axis and a vertical y axis was established. The point (0,0) or the center of the x and y coordinates was located at the location of the Sella for the lateral cephalometric radiograph and at the location of Crista Galli for the PA cephalometric radiograph. A red laser beam from the i-CAT Next Generation scanner (Imaging Sciences International, Hatfield, PA, USA) in line with the occlusal plane was used to keep the patient's head in a fixed position while the chin fits in the chin pad and the forehead is taped to the head rest of the machine.

Fifteen skeletal and dental cephalometric landmarks were chosen for each PA and lateral cephalometric radiograph derived from each CBCT scan (a total of 30 landmarks). Nine skeletal and six dental landmarks are going to be evaluated on each PA and lateral cephalometric radiograph. The cephalometric landmarks being used are summarized in Figure 5 and Table I.

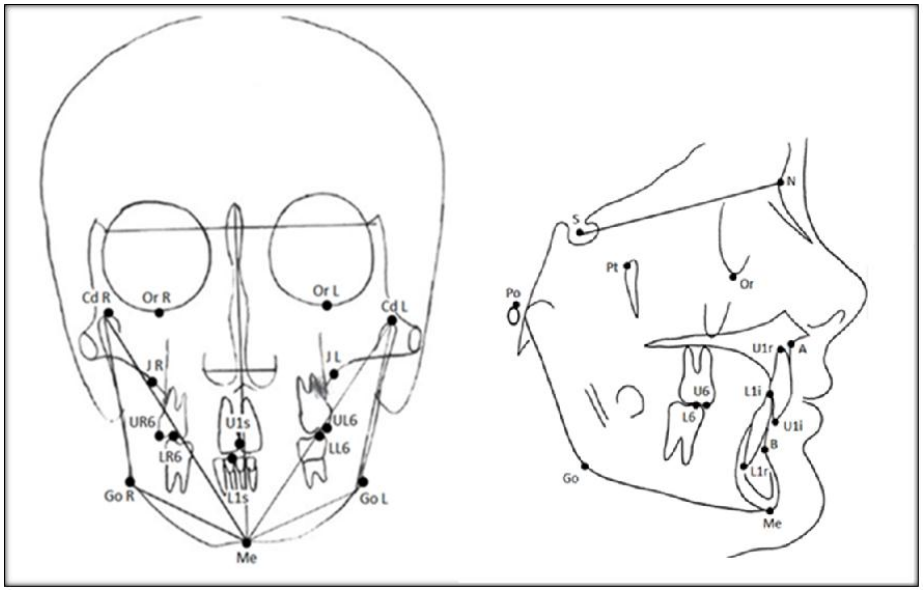

Figure 5. Lateral and PA cephalometric landmarks

TABLE I

LATERAL AND PA CEPHALOMETRIC LANDMARKS

Lateral Cephalometric Landmarks		Postero-anterior Cephalometric Landmarks	
Skeletal landmarks	**Dental landmarks**	**Skeletal landmarks**	**Dental landmarks**
Sella (S)	U1 tip (U1i)	Orbitale R (Or R)	U1s contact (U1s)
Nasion (N)	U1 root (U1r)	Orbitale L (Or L)	L1s contact (L1s)
Porion (Po)	L1 tip (L1i)	Jugal R (J R)	UR6 MB cusp (UR6)
Orbitale (Or)	L1 root (L1r)	Jugal L (J L)	UL6 MB cusp (UL6)
Pt point (Pt)	U6 MB cusp (U6)	Condylion R (Cd R)	LR6 MB cusp (LR6)
A point (A)	L6 MB cusp (L6)	Condylion L (Cd L)	LL6 MB cusp (LL6)
B point (B)		Gonion R (Go R)	
Gonion (Go)		Gonion L (Go L)	
Menton (Me)		Menton (Me)	

The tracings of the various compression rates were superimposed on Sella-Nasion (S-N) line to determine the accuracy of the identification of the landmarks and their location. Only a 1.5 mm deviation was accepted. Using the transfer structure function in Dolphin 3D imaging (Version 11.7, Dolphin Imaging, Chartsworth, CA), the S-N landmarks (in lateral radiograph) and Crista Gali perpendicular to Zygomatic left and right (in PA radiograph) were transferred throughout the series of 2D projections to ensure consistency in the reference plane for superimposition (orientation and registration).

Investigator 1 traced the landmarks on the iCAT 320 projections image described above for both the lateral and PA cephalogram; both X and Y coordinates were recorded for each landmark. Investigator 1 traced the same landmarks twice separated by one week to test the intra-observer reproducibility (Figure 6) performed by using the formula of the distance. This was done by taking the square of the difference between the x coordinate of the second time point (T2) and the x coordinate of the first time point (T1) for each landmark and adding the square of the difference between the y coordinate of the second time point (T2) and the y coordinate of the first time point (T1) and finally calculate the square root of the total: $\sqrt{[(x_2- x_1)^2+ (y_2- y_1)^2]}$

Investigator 2 traced the same landmarks on the five different constructed images for both the lateral and PA cephalograms twice separated by one week to test the intra-observer reproducibility in the same manner. Then, the data collected from investigator 1 were compared with the data collected from investigator 2 to test the inter-observer reproducibility by using the distance formula between the 2 investigators.

A clinically acceptable reference mean of 1.5 millimeters (mm) of accuracy was used. Therefore, if the absolute distance between landmark tracings was equal to 1.5 mm or was less than 1.5 mm, the landmark location was considered clinically accurate. This 1.5 mm margin of error is based on several studies that confirm this number as the reference mean used for accuracy. Baumrind and Frantz (1976) in their study on craniofacial growth prediction, superimposed lateral cephalograms on anterior cranial base using Sella-Nasion (S-N) line. They found an average positioning error of approximately 1.5 mm. This was also confirmed by Sagun et al (2012) who compared the relative accuracies of three computerized growth prediction

methods based on lateral cephalograms. That study showed a clinically acceptable range between 1.6 mm and 1.4 mm. Additionally, a study by Toepel-Sievers and Fischer-Brandies (1999), which tested the validity of Ricketts' growth prediction, considered length measurements to be clinically useful if the absolute error was less than 1.8 mm.

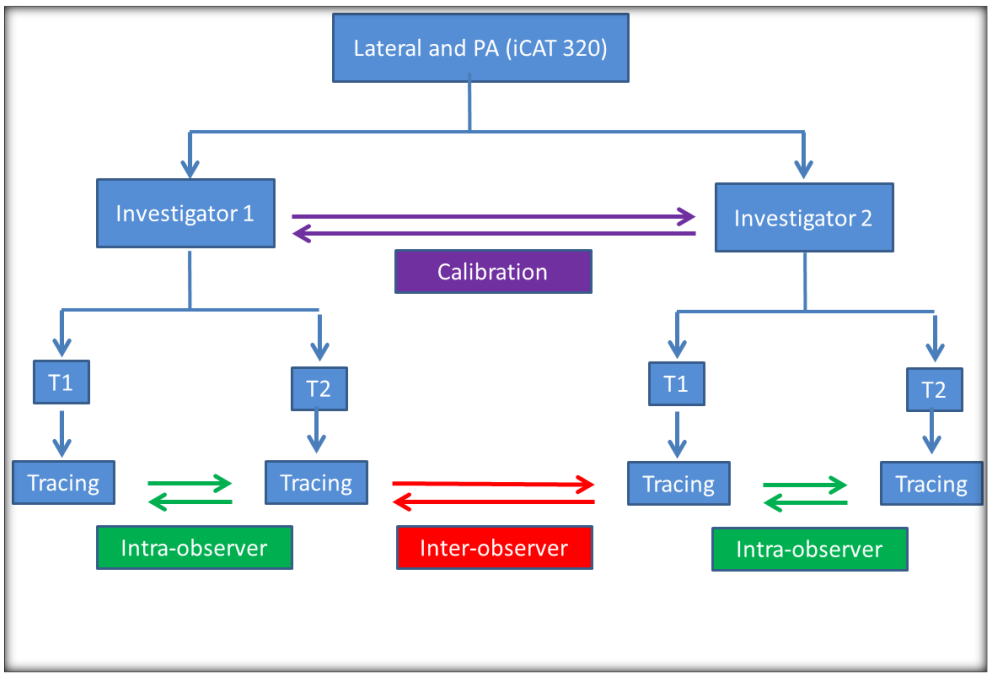

Figure 6. Reproducibility (accuracy)

Unfortunately, due to the constraint of sample size gathered during the time of the study, the inter and intra observer reliability cannot be statistically assessed. Therefore, only accuracy was used. Upon establishing the reproducibility and accuracy to the experiment, landmark identification among different compression projections for each single landmark on a given model was investigated. The five different compression rates for each one of the four different patients were traced in both lateral and PA cephalometric radiograph. Landmarks

were compared on both the x and y axes to the control (iCAT 320). The method is described in Figure 7.

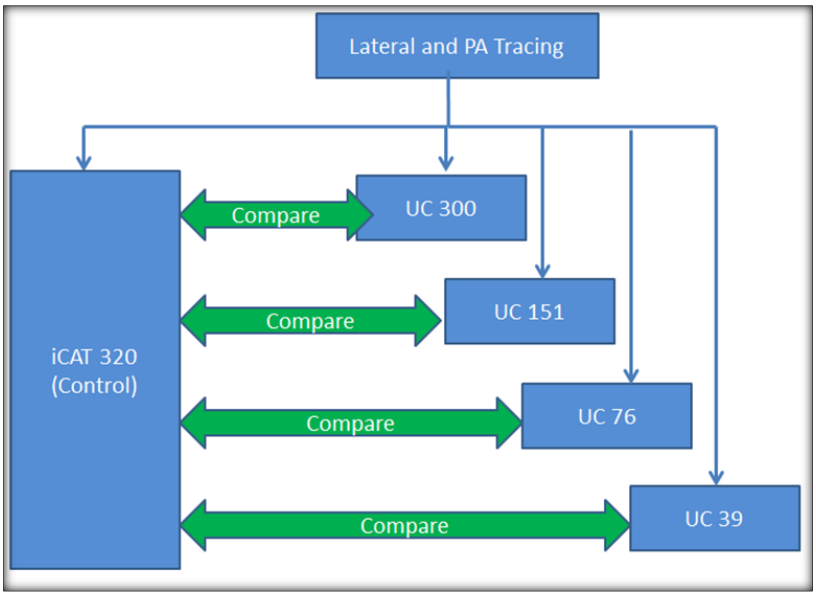

Figure 7. Comparisons between UC compressions and iCAT control

After the landmarks were traced, a spreadsheet was made of all values of x and y coordinates of the thirty landmarks. The values were filled in tables for lateral and PA cephalometric radiographs.

After all the measurements were obtained, landmark locations in the cephalograms derived from the UC compressions were compared to those of the iCAT 320 control. Then, the absolute distances between the landmarks of the compressions and those of the iCAT control were calculated (Dist). The distances between landmarks were added together for a single compression rate divided by the total number of the landmarks to calculate the average distance from the iCAT control.

3.4 Rational behind using the distance in measurements

Several ways were used to record the locations of different landmarks in this study. These include: the difference in the x coordinates of corresponding landmarks; the difference in the y coordinates of corresponding landmarks; and the absolute distance between the landmarks. All are relative to the iCAT control. Table II shows a small sample of the data collected from the lateral cephalometric radiograph of UC300 compression derived from the first model. Table II also shows the different ways of recording the locations of the cephalometric landmarks.

Regardless of how two landmarks are related to each other, the absolute distance is always longer than or equal to the horizontal or vertical projection. This is illustrated in Figure 8.

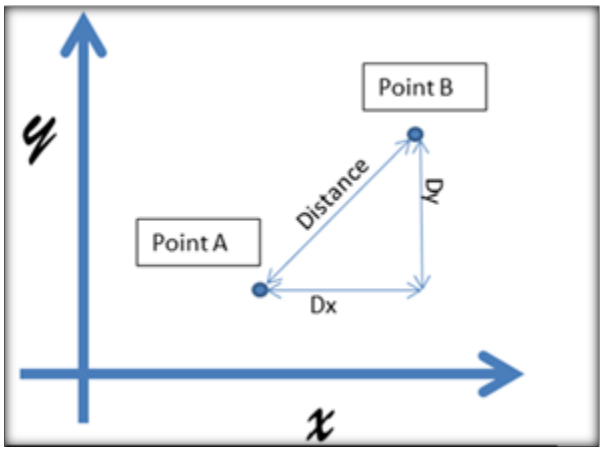

Figure 8. Measuring the distance

Therefore, using the distance to compare the accuracy of traced landmarks provides a protection against bias towards a tendency to show smaller values and therefore judging the landmarks on different lateral cephalometric images of different compression rates to be accurate based on those small values.

On the other hand, using the distance alone can be deceiving. Considering the distance only for the purposes of this project eliminates the effects of the horizontal and vertical differences (differences in x-coordinates and y-coordinates respectively) that can be significant in specific landmarks. Several landmarks, by definition, show high accuracy only in one dimension while a wide range of values can be observed in the other dimension. Point B for example shows more vertical than horizontal variability. This is illustrated in figure 9.

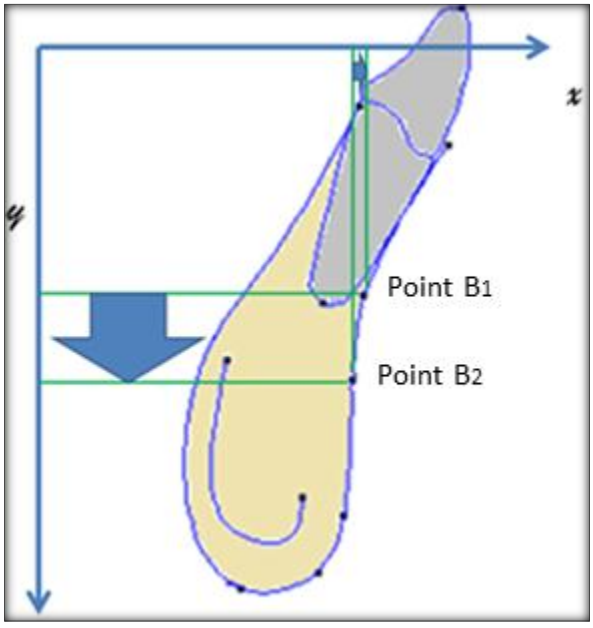

Figure 9. Horizontal and vertical variability of Point B

If only the x-coordinate of Point B was used to determine the accuracy of the image, Point B would show a very high accuracy when comparing different cephalometric images of different compression rates. On the other hand, if only the y-axis were used, Point B would show a lower accuracy value. The opposite can be seen in other points like Menton for example where the vertical dimension is limited.

SNB angle (Sella-Nasion-Point B angle) is commonly used in orthodontics to evaluate the sagittal location of the mandible in relation to the anterior cranial base (Sella-Nasion line). As illustrated in figure 10, the horizontal component of Point B is more important because of its larger effect on the measurement of SNB angle compared with the effect of its vertical component. Therefore it is important to understand these differences that are inevitable in the process of tracing regardless of the image quality.

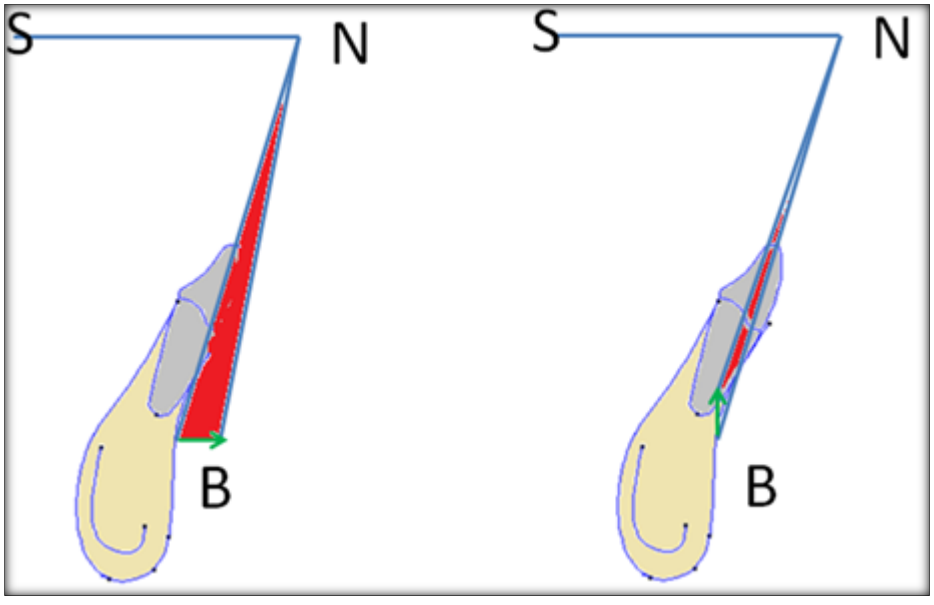

Figure 10. Influence of Point B on the SNB angle

In conclusion, using the distance between cephalometric landmarks to evaluate the accuracy of the tracings can be very helpful because it provides an objective method of determining the quality of lateral and PA cephalometric radiographs derived from different compression rates of CBCT images. However, this can lead to loss of significant amount of information about how the landmarks perform in a horizontal or vertical manner.

3.5 Descriptive findings

This feasibility study consists of four units of analysis (images) to be evaluated. Using Kolmogorov-Smirnov and Shapiro-Wilk test, raw data of these four images involved in the study showed a normal distribution data set for the seven out of eight UC compressions analyzed, (Table II). The only compression that did not show a normal distribution was the Lateral Cephalogram UC76.

TABLE II

TESTS OF NORMALITY

	Kolmogorov-Smirnov[a]			Shapiro-Wilk		
	Statistic	df	Sig.	Statistic	df	Sig.
Lateral ceph 300i	.263	4	.	.887	4	.370
Lateral ceph 151i	.297	4	.	.765	4	.053
Lateral ceph 76i	.408	4	.	.706	4	.014
Lateral ceph 39i	.220	4	.	.948	4	.701
PA ceph 300i	.250	4	.	.908	4	.472
PA ceph 151i	.245	4	.	.871	4	.303
PA ceph 76i	.243	4	.	.967	4	.822
PA ceph 39i	.203	4	.	.956	4	.757

a. Lilliefors Significance Correction (Majority are normally distributed except Lateral Ceph UC76)

Based only on the four images, similar results were found testing with parametrics and non parametrics statistics. The following tables show results of the pairs compared using Paired Student t-test. Note that the purpose of this project is not to compare between all the different combinations of pairs of the UC compression rates. Only those compressions that follow one another are being compared without including distant compressions. For example the UC300 compression is not being compared with the UC39 compression. The UC300 compression is being compared with UC151 compression and the UC39 compression with the UC76 compression, (Tables III- IV).

TABLE III

SUMMARY DESCRIPTIVE OF THE PAIRED SAMPLES

		Mean	N	Std. Deviation	Std. Error Mean
Pair 1	Lateral ceph 300i	.7100	4	.09764	.04882
	Lateral ceph 151i	.8350	4	.13868	.06934
Pair 2	Lateral ceph 151i	.8350	4	.13868	.06934
	Lateral ceph 76i	1.1275	4	.25250	.12625
Pair 3	Lateral ceph 76i	1.1275	4	.25250	.12625
	Lateral ceph 39i	1.0325	4	.27035	.13518
Pair 4	PA ceph 300i	.7200	4	.17146	.08573
	PA ceph 151i	.8475	4	.23852	.11926
Pair 5	PA ceph 151i	.8475	4	.23852	.11926
	PA ceph 76i	1.0050	4	.30447	.15223
Pair 6	PA ceph 76i	1.0050	4	.30447	.15223
	PA ceph 39i	1.2475	4	.31889	.15945

TABLE IV

PAIRED SAMPLES STATISTICS

		Paired Differences			
		Mean	Std. Deviation	95% Confidence Interval of the Difference	95% Confidence Interval of the Difference
				Lower	Upper
Pair 1	Lateral ceph 300i - Lateral ceph 151i	-.12500	.14754	-.35976	.10976
Pair 2	Lateral ceph 151i - Lateral ceph 76i	-.29250	.35425	-.85619	.27119
Pair 3	Lateral ceph 76i - Lateral ceph 39i	.09500	.33611	-.43982	.62982
Pair 4	PA ceph 300i - PA ceph 151i	-.12750	.15196	-.36930	.11430
Pair 5	PA ceph 151i - PA ceph 76i	-.15750	.24199	-.54256	.22756
Pair 6	PA ceph 76i - PA ceph 39i	-.24250	.29545	-.71263	.22763

By examining the distribution of the raw data based only on four images, the variables being investigated in this study, reveals that preliminary results showed no mean differences at each pair in consideration. Therefore the lowest compression rate (UC39) can still be used to perform accurate cephalometric analysis for orthodontic purposes.

In the study conducted by Baumrind and Frantz (1971), the results showed that errors in landmark identification are too great to be ignored even when tracing the same lateral cephalometric images. But again, unexperienced first year orthodontic residents were asked to

trace the images in their study. This might contribute to the magnitude of errors we see in that study. They also found that the magnitude of error varies greatly from landmark to landmark. This is illustrated on table V.

TABLE V

ESTIMATING ERRORS BY BAUMRIND AND FRANTZ (1971)

SKELETAL LANDMARKS	**MEAN ESTIMATING ERROR**
1. Porion	0.39 +/- 0.13
2. Sella	0.48 +/- 0.14
3. Nasion	0.73 +/- 0.52
4. Menton	1.00 +/- 0.36
5. Point A	1.00 +/- 0.37
6. Pogonion	1.06 +/- 0.36
7. Orbitale	1.09 +/- 0.65
8. Point B	1.27 +/- 0.60
9. Gonion (U)	3.48 +/- 1.12
10. Gonion (L)	3.75 +/- 1.10
DENTAL LANDMARKS	
1. Upper 1 edge	0.37 +/- 0.11
2. Lower 1 edge	0.44 +/- 0.19
3. Upper 1 apex	0.98 +/- 0.50
4. Lower 6 cusp (L)	1.05 +/- 0.50
5. Lower 6 cusp (R)	1.32 +/- 0.59
6. Lower 1 apex	1.74 +/- 0.59

4. RESULTS

4.1 Results

Table VI exhibits data collected from the lateral cephalometric radiograph of UC300 compression derived from the first model. The data shows absolute values of x coordinates and y coordinates of both iCAT and UC300 compression, the differences in x coordinates and y coordinates, and the absolute distances.

TABLE VI

SAMPLE BASED ON Four IMAGE THE DATA

		iCAT 1			UC300					
	Landmark Name		X	Y		X	Y	Dx	Dy	Dist
1	A Point		47.6	-35.9		47.8	-35.6	0.2	0.3	0.3
2	B Point		49.0	-72.6		49.7	-73.5	0.7	-0.9	1.1
3	Gonion		-3.7	-60.0		-2.7	-61.6	0.9	-1.6	1.9
4	L1 Root		47.0	-71.6		47.8	-72.0	0.8	-0.5	1.0
5	L1 Tip		54.9	-54.6		55.3	-54.9	0.5	-0.3	0.5
6	L6 Occlusal		34.7	-53.4		35.3	-54.7	0.6	-1.3	1.4
7	Menton		42.2	-87.8		41.3	-87.9	-0.8	-0.1	0.8
8	Nasion		50.1	10.2		50.0	10.2	-0.1	0.0	0.1
9	Orbitale		42.7	-12.6		43.0	-12.8	0.2	-0.2	0.3
10	PT Point		11.0	-10.7		10.9	-12.4	-0.1	-1.7	1.7
11	Porion		-18.7	-10.8		-18.7	-11.1	0.1	-0.3	0.3
12	Sella		0.0	0.0		0.0	0.0	0.0	0.0	0.0
13	U1 Root		46.1	-38.5		46.2	-37.6	0.1	0.8	0.8
14	U1 Tip		55.0	-53.4		55.5	-53.7	0.4	-0.3	0.5
15	U6 Occlusal		32.3	-53.0		32.8	-53.8	0.4	-0.8	1.0

The major indicator used in this study to compare and determine the accuracy of the landmarks was the distance between the landmarks of the UC compressions and the corresponding landmarks in the iCAT control (Dist).

After calculating all the distances of the landmarks (see last column in table VII), the average value of the distances and the standard deviations were calculated for every single

compression on the lateral cephalometric radiographs for the 3D images of patients (3D models). The same procedure was performed for the PA cephalometric radiograph. The results are demonstrated in Table VII and Figure 11.

TABLE VII

SUMMARY OF PRELIMINARY STATISTICS

Lateral cephalometric landmarks					
Reconstruction rate		300	151	76	39
Average	Model 1	1.10	1.11	1.06	1.26
	Model 2	1.08	0.97	1.45	1.33
	Model 3	0.87	1.05	1.61	1.28
	Model 4	1.09	1.17	1.66	1.50
	Mean	1.04	1.07	1.44	1.34
SD	Model 1	0.71	0.67	0.95	0.83
	Model 2	0.75	0.50	0.57	0.68
	Model 3	0.54	0.77	0.99	1.23
	Model 4	0.71	0.80	0.92	1.21
	Mean	0.68	0.68	0.86	0.99
Mode	Model 1	0.80	0.90	0.50	0.70
	Model 2	0.70	1.00	1.20	0.80
	Model 3	0.40	0.70	0.90	0.60
	Model 4	0.80	1.00	1.60	0.50
	Mean	0.68	0.90	1.05	0.65
Max	Model 1	3.40	3.20	5.80	4.90
	Model 2	3.10	2.70	2.80	3.10
	Model 3	2.20	3.70	5.00	5.10
	Model 4	3.40	3.20	5.10	5.30
	Mean	3.03	3.20	4.68	4.60
Min	Model 1	0.00	0.00	0.00	0.00
	Model 2	0.00	0.00	0.00	0.00
	Model 3	0.00	0.00	0.00	0.00
	Model 4	0.00	0.00	0.00	0.00
	Mean	0.00	0.00	0.00	0.00

Postero-anterior cephalometric landmarks					
Reconstruction rate		300	151	76	39
Average	Model 1	0.96	1.18	1.40	1.56
	Model 2	0.57	0.86	0.66	1.21
	Model 3	0.63	0.66	0.95	0.82
	Model 4	0.72	0.69	1.01	1.40
	Mean	0.72	0.85	1.00	1.25
SD	Model 1	0.89	0.55	0.93	0.91
	Model 2	0.62	0.65	0.61	0.91
	Model 3	0.40	0.42	1.15	0.73
	Model 4	0.77	0.54	0.80	1.26
	Mean	0.67	0.54	0.87	0.95
Mode	Model 1	0.60	1.10	1.00	1.20
	Model 2	0.30	0.70	0.70	0.70
	Model 3	0.70	0.40	0.90	0.60
	Model 4	0.30	0.40	0.60	0.60
	Mean	0.48	0.65	0.80	0.78
Max	Model 1	3.40	2.20	3.90	4.20
	Model 2	2.60	2.80	2.50	3.00
	Model 3	1.60	1.70	4.70	2.50
	Model 4	3.10	2.30	3.50	4.80
	Mean	2.68	2.25	3.65	3.63
Min	Model 1	0.00	0.00	0.00	0.00
	Model 2	0.00	0.00	0.00	0.00
	Model 3	0.00	0.00	0.00	0.00
	Model 4	0.00	0.00	0.00	0.00
	Mean	0.00	0.00	0.00	0.00

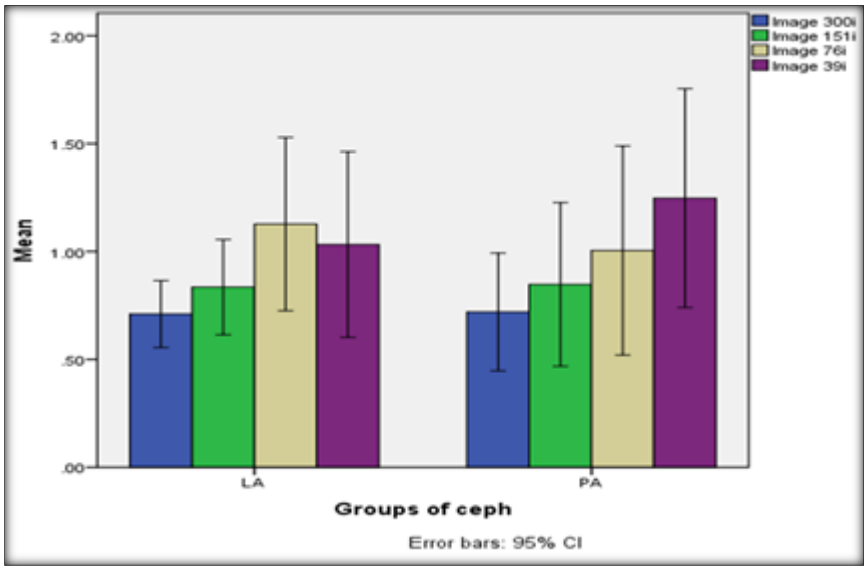

Figure 11. Summary of preliminary statistics

The average distance between the landmarks show a gradual increase when moving through the compressions starting from UC300 to UC39. The only exception is between UC76 and UC39 on the lateral cephalometric tracing where the UC39 shows shorter average distance than the UC76. Even though UC39 shows shorter average when compared to UC76, the standard deviation is larger for the UC39. Furthermore, one has to keep in mind the small sample size used to conduct this feasibility study.

Many landmarks showed distances that exceeded the 1.5 mm error margin when compared to the iCAT control and hence considered inaccurate according to our standards. However, when the average is calculated for all the landmarks of a single compression rate, the results show that none of the compression rates exceeded the 1.5 mm limit. This is illustrated in Figure 11. This indicates that all the compression rates are valid for tracing and cephalometric analysis.

When analyzing the maximum distance found between the landmarks of the compression and those of the iCAT control, it is expected that the maximum distance would increase when moving from higher quality images (UC300) to lower quality images (UC39) where the poor quality makes it much harder to accurately trace the landmarks resulting in longer distances between the corresponding landmarks. The results in this study confirm this in the lateral cephalometric values except for a small insignificant difference between the UC76 and UC39 measurements. When looking at the PA cephalometric values, a big discrepancy is observed between the UC300 and UC151. Again, realizing that the sample size used in this project is smaller than what is required for more definitive conclusions. Another issue is that orthodontic residents are not well-trained in tracing PA cephalometric radiographs. Unlike the lateral cephalometric analysis, the PA cephalometric analysis is not a routine record in the diagnosis and treatment planning of patients.

5. DISCUSSION

Lateral and PA cephalometric radiographs are among the most important diagnostic records influencing the process of comprehensive diagnosis and treatment planning in orthodontic practices. Accurate cephalometric analysis obtained from utilizing high quality lateral and PA cephalograms is a must for a successful determination of patients underlying skeletal or dental discrepancy contributing to a particular malocclusion. Mistakes in diagnosis and treatment planning as a result of ignoring the cephalometric analysis or poor landmark identification are not uncommon in orthodontic practices.

Reducing the number of 2D projections needed to reconstruct the 3D images can be very useful in reducing the unnecessarily high radiation dose orthodontic patients are exposed to in orthodontic practices taking CBCT images. However, this reduction in the radiation exposure should not be carried out on the expense of the quality of the images needed for a proper diagnosis and treatment planning.

The results of this project show a very promising reduction of the number of 2D projections needed to construct the iCAT 3D images. Therefore, a significant reduction in the radiation dose was obtained without dramatic negative effects on the accuracy of landmark identification and cephalometric analysis.

5.1 Using the average for measurements.

Calculating the average can help simplifying the process of analysis especially when a large amounts of data need to be analyzed. It is often tempting to overlook the many details you find in your data and rely on the mean value to derive your conclusion. However, by doing this, a large amount of information can be very easily obscured and unconsciously deviate the argument into a totally different direction than what is the data really illustrates.

As illustrated in Figure 11 and Figure 12a , none of the lateral or PA cephalometric radiographs derived from different UC compressions show a value that exceeds the 1.5mm error margin. But when looking at the original data used to calculate the average, some data actually exceeded the 1.5 mm margin (Figure 12b).

Furthermore, one column of the data illustrated in figure 12 can be further broken down into more detailed data. Every column in figure 12 represents the average of all the landmarks used to calculate the data of a specific orientation (lateral or PA) of a specific model (1, 2, 3, and 4) using a specific compression (UC300, UC151, UC76, UC39). Figure 13 shows the detailed data of landmarks contained in the lateral cephalometric radiograph of model 3 using a compression rate of UC300. Evident in this column of data, even though the mean of the landmarks in this data set is far below the 1.5mm limit, some individual landmark distances used to calculate the mean exceed the limit.

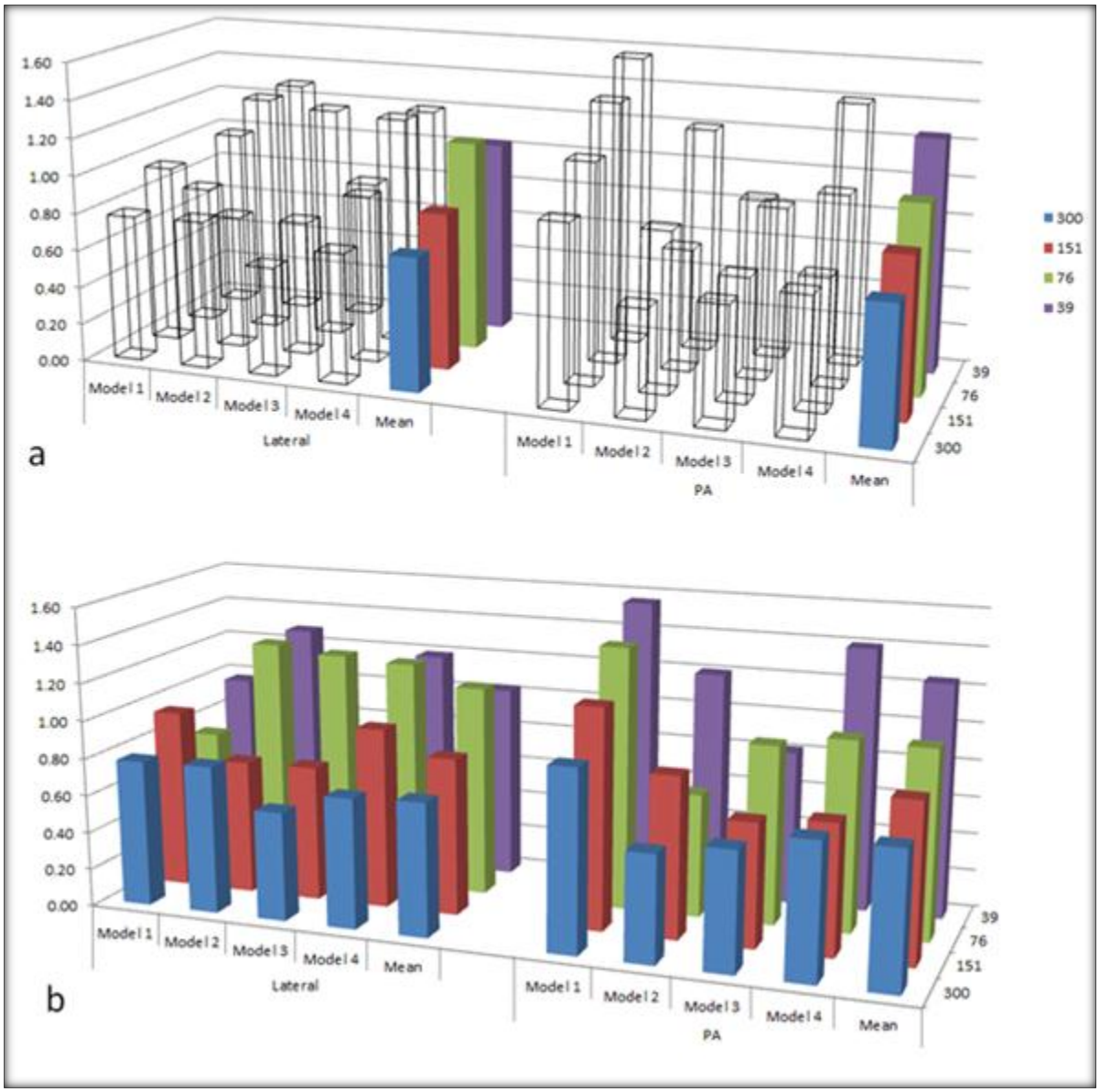

Figure 12. a) Summary of the mean values (n=4), b) mean values and the original data.

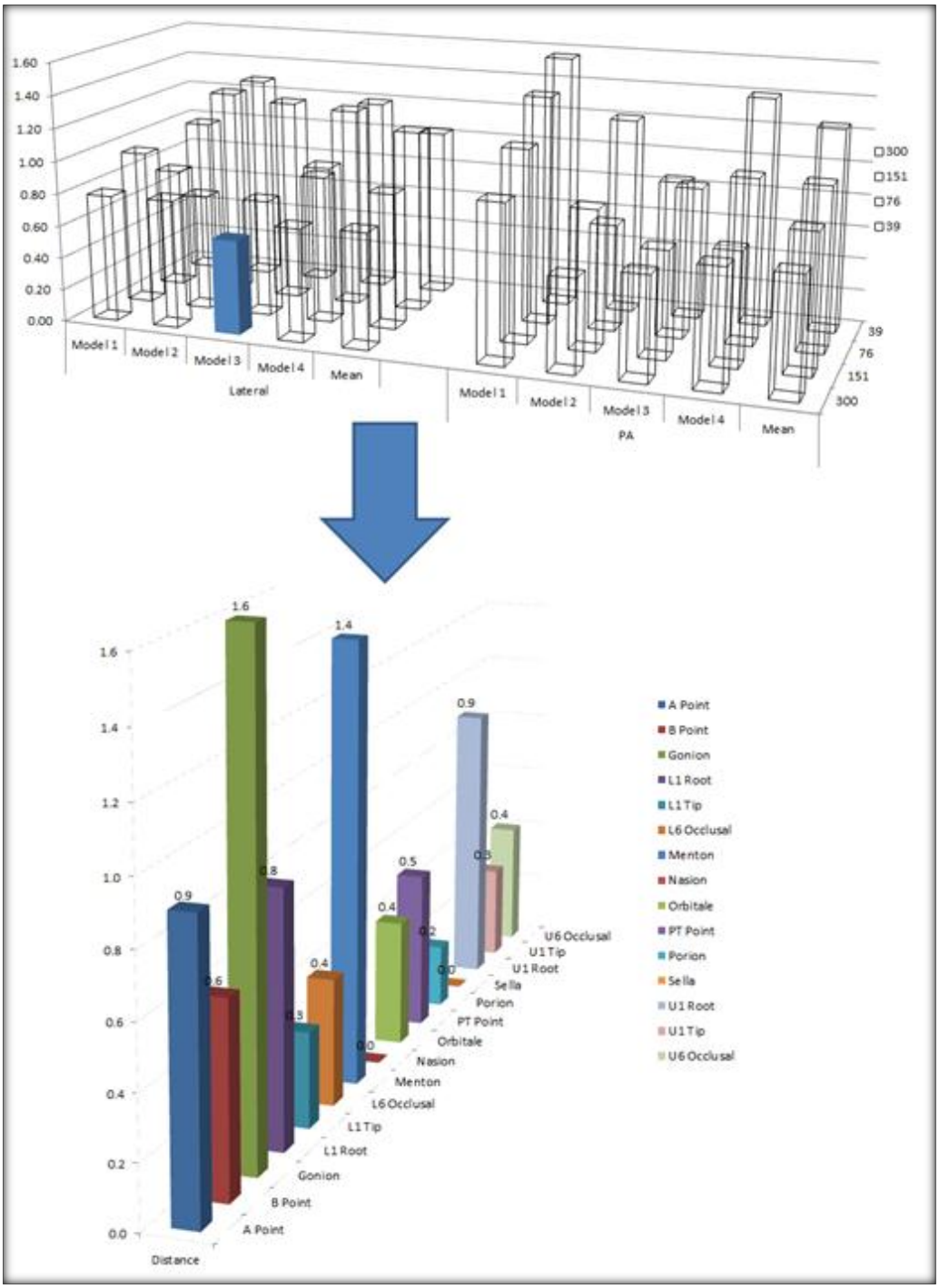

Figure 13. Breaking the data sets into the original landmarks

In conclusion, looking at the mean values in figure 11, one can easily assume that none of the landmarks exceeded our accuracy limit of 1.5mm. However, many of these landmarks actually did. Using the average alone to describe the data can lead to false perceptions.

As discussed before and shown in figure 5 and table I, only 15 landmarks were selected and used in the lateral cephalometric analysis. In a separate data sheet, the original 65 lateral cephalometric landmarks were used as well. The same conclusion was derived from this data set but with larger standard deviation. This confirms the preliminary results we obtained.

5.3 Limitations

As discussed in the statistics section, a larger sample size can vastly expand the number of ideas for potential studies that can be conducted using this technology. A suitable sample size can be used to evaluate specific landmarks individually to identify the landmarks with predictable and reproducible positions that can be used further for cephalometric analyses and superimpositions to evaluate growth or treatment progress. Moreover, good data can use different variables to compare compression rates, specific age groups, and specific cephalometric measurements.

Using the distance to evaluate the accuracy and the quality of the tracing has its strength and its weaknesses. The distance is one of the most easily calculated and reliable measurements. It can be easily understood among most orthodontists. However, many landmarks are more predictable in one dimension in comparison to the other and therefore it is

important to account for these differences. Using the absolute distance without any considerations for the direction of the discrepancy can be deceiving at the time of the data analysis.

Because of the large number of measurements being conducting in this study, using the average or the mean to simplify the data seems ideal. However, one needs to be aware of the many side effects of using such protocol in the interpretation of the data by the clinician and the researcher.

The order in which the tracings are performed can influence the results tremendously. In this project, lateral and PA cephalometric radiographs were traced starting with the lowest compression rate first followed by the next up to the iCAT control. This was performed to prevent the good quality of the higher compression rate images from influencing the process of landmark identification of the lower compression rates. Unfortunately, bias still exist in this situation because all the images of the same patient were traced together. A better method of choosing the order of the tracings is to mix different patients and compressions together and trace them in a more randomized order to eliminate this kind of bias. This can be more successful with a bigger sample size.

5.3 Further Research

This project is a feasibility study for future studies that can be performed in the field of cephalometrics derived from 3D CBCT and landmark identification. These data can be used to perform a comprehensive comparison between variables in many ways including calculating the actual sample size for future similar studies. A study can be designed to compare how individual landmarks perform on a scale of accuracy when traced on different cephalometric radiographs derived from different numbers of projections. This can be done to find those landmark or landmarks that remain accurate even when traced on much lower quality compressions. The same method can be used to determine the least reliable cephalometric landmarks when going down beyond a specific compression rate.

In this study, a lateral cephalometic grid was used with its center in Sella to assign an x and y coordinate for each single landmark. Crista Galli was used as the center for the postero-anterior ceph in a similar way. With the assistance of more developed software, one can very easily establish a 3D grid with x,y, and z axis with one point as the center of the triad (0,0,0) so that the lateral cephalometric landmarks can be verified with the assistance of the PA cephalograms or any other views. This can be done on landmarks that are common on both lateral and PA cephalograms. Examples would be Menton, incisal edges and root tips, ANS, and others. Some points can be seen as bilateral structures on PA and lateral cephalometrics such as Gonion, Anti-gonial notch, Orbitale, Condylion, Porion, and others. These points can be verified more easily if the investigator has a complete control of the orientation of the 3D image while tracing the images. Moreover, a comprehensive 3D image tracing by establishing

bony landmarks on the surface of the skull as if you are holding a dry skull in your hands with the ability of virtually dissect the skull to visualize internal structure also is not far in the distant future. As discussed before, Baumrind et al (1976) talked about the errors of projective displacement. Baumrind et al also said that this kind of errors can be eliminated only by developing some practical method of 3D measurement. The CBCT technology wasn't available at Baumrind time but he predicted that someday the ability of orienting the 3D volume before projecting it into 2D image will be possible. He also described, in his work on craniofacial growth prediction, different ways of superimposition and made a distinction between mathematical best fit and biologic best fit. Using different plans for superimposition was also discussed.

Increasing the sample size in future research would improve the strength of the study and open the opportunity for more ways of analyzing the 3D images and landmarks. The increased amount of literature in the field of 3D imaging available makes one realize how much potential this technology can offer. In the near future, orthodontics is going to look much different than what is available at the present. Moreover, what is being taught in orthodontic programs today as the standard, which is a 2D analysis with all of its deficiencies would be changed in the future.

Furthermore, new reconstruction algorithms are being designed with lower radiation exposure to the patient and higher quality reconstruction of CBCT scans. This might change the orthodontic practice tremendously. Other methods of reducing the radiation dose, discussed previously, should be utilized and tested. In the near future, CBCT will be safer and more

efficient. The radiation exposure to our patient might even go down below the level of the radiation dose of today's conventional 2D imaging. When this happen, more and more analyses will be created for a comprehensive 3D diagnosis and treatment planning. This will open the chance for more research ideas and new methods of using this technology.

6. CONCLUSION

By examining the distribution of the raw data based on the variables being investigated in this study, the data showed preliminary results that there is no statistically significant mean difference when comparing the means of distances between the average locations of different landmarks in lateral and PA cephalometric radiographs derived from CBCT images of different compression rates when compared consecutively.

Although only a few individual landmarks exceeded the 1.5 mm error margin set to evaluate the accuracy of the tracing, none of the means of the landmarks in different compressions rates in both lateral and PA cephalometric radiographs exceeded the 1.5 mm error margin.

More research projects with larger samples need to be conducted to define the few landmarks that introduced errors in the measurements. Also, the reasons behind these errors should be identified and then a solution can be suggested to improve the tracing process.

Therefore, an accurate tracing of landmarks can be accomplished even when using the low quality UC39 projections data when compared to the iCAT 320 projections data. If the UC39 compression is good enough to derive accurate cephalometric results, then why expose the patients to an unnecessarily high radiation dose to obtain a higher quality image?

These findings, together with other similar studies using larger sample size and more defined criteria, can influence the CBCT imaging companies to adjust the radiation dose and time of exposure at least for orthodontic offices to more accurately reflect the needs of

orthodontic use of the CBCT scans. For the present time, taking a full CBCT scans routinely for orthodontic patients is still unjustified. If only a 2D lateral cephalometric radiograph is needed for diagnosis and treatment planning, the radiation from a CBCT must not be greater than that of the conventional 2D radiographs.

LITERATURE CITED

Araki K, Maki K, Seki K, Sakamaki K, Harata Y, Sakaino R, Okano T, Seo K. Characteristics of a newly developed dentomaxillofacial X-ray cone beam CT scanner (CB MercuRay): system configuration and physical properties. Dentomaxillofac Radiol 2004; 33: 51-59.

Baumrind, S., Frantz, R.: The reproducibility of head film measurements: 1. Landmark identification. Am J Orthod. 60:111-126, 1971.

Baumrind S, Miller D, Molthen R. The reliability of head film measurements. 3. Tracing superimposition. Am J Orthod. 1976;70(6):617-44.

Brooks SL. CBCT dosimetry: orthodontic considerations. Seminars in Orthodontics. Jun 2009;15(1):14-18.

Brown AA, Scarfe WC, Scheetz JP, Silveira AM, Farman AG. Linear accuracy of cone beam CT derived 3D images. Angle Orthod 2009; 79: 150-157.

Choi, K., Wang, J., Zhu, L., Suh, T.S., Boyd, S., Xing, L.: Compressed sensing based cone-beam computed tomography reconstruction with a first-order methoda. Medical Physics. 2010; 37 (9):5113-5125.

Emil YS; Yuval D; Ingrid R; Christer U; Xiaochuan P. Optimizing algorithm parameters based on a model observer detection task for image reconstruction in digital breast tomosynthesis. IEEE Nuclear Science Symposium Conference Record. 2012:4230-4232:[6153811].

Geijer H, Norrman E, Persliden J. Optimizing the tube potential for lumbar spine radiography with a flat-panel digital detector. Br J Radiol 2009; 82: 62-68

Grünheid T, Kolbeck schieck JR, Pliska BT, Ahmad M, Larson BE. Dosimetry of a cone-beam computed tomography machine compared with a digital x-ray machine in orthodontic imaging. Am J Orthod Dentofacial Orthop. 2012;141(4):436-43.

Gwen RJS, Filip S , Jarg-Erich H. Three-Dimensional Cephalometry ,A Color Atlas and Manual. Pages 7-11. Library of Congress Control Number: 2005929880 (2005)

Han X, Bian J, Eaker DR, et al. Algorithm-enabled low-dose micro-CT imaging. IEEE Trans Med Imaging. 2011;30(3):606-20.

Hashimoto K, Arai Y, Iwai K, Araki M, Kawashima S, Terakado M. A comparison of a new limited cone beam computed tomography machine for dental use with a multidetector row helical CT machine. Oral Surg Oral Med Oral Pathol Oral Radiol Endod 2003; 95: 371-377.

Hassan B, Van der stelt P, Sanderink G. Accuracy of three-dimensional measurements obtained from cone beam computed tomography surface-rendered images for cephalometric analysis: influence of patient scanning position. Eur J Orthod. 2009;31(2):129-34.

Hatcher DC. Operational principles for cone-beam computed tomography. J Am Dent Assoc. 2010;141 Suppl 3:3S-6S.

Horner K. Review article: radiation protection in dental radiology. Br J Radiol 1994; 67: 1041-1049.

International Commission on Radiation Units and Measurements (ICRU).Options for Characterizing Energy Deposition. Journal of the ICRU Vol 11 No 2 (2011) Report 86

Kalender WA, Kyriakou Y. Flat-detector computed tomography (FD-CT). Eur Radiol. 2007; 17: 2767-2779.

Kwong JC, Palomo JM, Landers MA, Figueroa A, Hans MG. Image quality produced by different cone-beam computed tomography settings. Am J Orthod Dentofacial Orthop. 2008; 133: 317-327.

Larson BE. Cone-beam computed tomography is the imaging technique of choice for comprehensive orthodontic assessment. Am J Orthod Dentofacial Orthop. 2012;141(4):402, 404, 406 passim.

Liang, X., Lambrichts, I., Sun, Y., Denis, K., Hassan, B., Li, L., Pauwels, R., Jacobs, R. (2010). A comparative evaluation of Cone Beam Computed Tomography (CBCT) and Multi-Slice CT (MSCT). Part II: On 3D model accuracy. European Journal of Radiology, 75 (2), 270-274.

Liedke GS, da Silveira HE, da Silveira HL, Dutra V, de Figueiredo JA. 2009. Influence of voxel size in the diagnostic ability of cone beam tomography to evaluate simulated external root resorption. J Endod 2009; 35: 233-235.

Lofthag-Hansen.Cone Beam Computed Tomography. Radiation Dose and Image Quality assessments. PhD thesis 2010: Sahlgrenska Academy, University of Gothenburg.

Lofthag-Hansen S, Thilander-Klang A, Ekestubbe A, Helmrot E, Gröndahl K. Calculating effective dose on a cone beam computed tomography device: 3D Accuitomo and 3D Accuitomo FPD. Dentomaxillofac Radiol 2008; 37: 72-79

Lofthag-Hansen S, Thilander-Klang A, Gröndahl K. Evaluation of subjective image quality in relation to diagnostic task for cone beam computed tomography with different fields of view. Eur J Radiol. 2010: Oct 19. [Epub ahead of print]

Loubele M, Bogaerts R, Van Dijck E, Pauwels R, Vanheusden S, Suetens P, Marchal G, Sanderink G, Jacobs R. Comparison between effective radiation dose of CBCT and MSCT scanners for dentomaxillofacial applications. Eur J Radiol. 2009; 71: 461-468.

Ludlow JB, Davies-Ludlow LE, Brooks SL. Dosimetry of two extraoral direct digital imaging devices: NewTom cone beam CT and Orthophos Plus DS panoramic unit. Dentomaxillofac Radiol 2003; 32: 229-234.

Ludlow JB, Davies-Ludlow LE, Brooks SL, Howerton WB. Dosimetry of 3 CBCT devices for oral and maxillofacial radiology: CB Mercuray, NewTom 3G and i-CAT. Dentomaxillofac Radiol 2006; 35: 219-226

Ludlow JB, Ivanovic M. Comparative dosimetry of dental CBCT devices and 64-slice CT for oral and maxillofacial radiology. Oral Surg Oral Med Oral Pathol Oral Radiol Endod 2008; 106:106-114.

Ludlow JB, Davis-Ludlow LE, White SC. Patient risk related to common dental radiographic examinations: The impact of 2007 International Commission on Radiological Protection recommendations regarding dose calculation. JADA 2008; 139: 1237-1243

Pasini A, Casali F, Bianconi D, Rossi A and Bontempi M. A new cone-beam computed tomography system for dental applications with innovative 3D software. Int J CARS 2007;1: 265-273.

Patcas R, Müller L, Ullrich O, Peltomäki T. Accuracy of cone-beam computed tomography at different resolutions assessed on the bony covering of the mandibular anterior teeth. Am J Orthod Dentofacial Orthop. 2012;141(1):41-50.

Pauwels R, Beinsberger J, Collaert B, Theodorakou C, Rogers J, Walker A, Cockmartin L, Bosmans H, Jacobs R, Bogaerts R, Horner K The SEDENTEXCT Project Consortium.

Effective dose range for dental cone beam computed tomography scanners. Eur J Radiol. 2010 Dec 31. [Epub ahead of print]

Pauwels R, Stamatakis H, Manousaridis G, et al. Development and applicability of a quality control phantom for dental cone-beam CT. J Appl Clin Med Phys. 2011;12(4):3478.

Qu XM, Li G, Ludlow JB, Zhang ZY, Ma XC. Effective radiation dose of ProMax 3D cone-beam computerized tomography scanner with different dental protocols. Oral Surg Oral Med Oral Pathol Oral Radiol Endod. 2010; 110: 770-6.

Roberts JA, Drage NA, Davies J, Thomas DW.Effective dose from cone beam CT examinations in dentistry. Br J Radiol 2009; 82: 35-40.

Sagun M, Kusnoto B, Evans C, Galang T, Obrez A, Viana G. Assessment of Computerized Cephalometric Growth Prediction: A Comparison of Three Methods. MAI/ 50-06, Jun 2012. 1513864.

Scarfe, William C., and Allan G. Farman. 2008. "What is Cone-Beam CT and How Does it Work?" Dental Clinics of North America no. 52 (4):707-730. doi: http://dx.doi.org/10.1016/j.cden.2008.05.005.

Sur J, Seki K, Koizumi H, Nakajima K, Okano T. Effects of tube current on cone-beam computerized tomography image quality for presurgical implant planning in vitro. Oral Surg Oral Med Oral Pathol Oral Radiol Endod. 2010; 110: e29-33

Toepel-Sievers C, Fischer-Brandies H: Validity of the computer-assisted cephalometric growth prognosis VTO (Visual Treatment Objective) according to Ricketts. J Orofac Orthop; 1999;60(3):185-94

Tsiklakis K, Donta C, Gavala S, Karayianni K, Kamenopoulou V, Hourdakis CJ. Dose reduction in maxillofacial imaging using low dose Cone Beam CT. Eur J Radiol 2005; 56: 413-417.

Vandenberghe B, Jacobs R, Yang J: Diagnostic validity (or acuity) of 2D CCD versus 3D CBCT-images for assessing periodontal breakdown. Oral Surg Oral Med Oral Pathol Oral Radiol Endod. 2007; 104(3):395-401.

Van Vlijmen OJ, Maal T, Bergé SJ, Bronkhorst EM, Katsaros C, Kuijpers-Jagtman AM.A comparison between 2D and 3D cephalometry on CBCT scans of human skulls.Int J Oral Maxillofac Surg2010;39:156–160.

Van Vlijmen OJ, Bergé SJ, Bronkhorst EM, Swennen GR, Katsaros C, Kuijpers-jagtman AM. A comparison of frontal radiographs obtained from cone beam CT scans and conventional frontal radiographs of human skulls. Int J Oral Maxillofac Surg. 2009;38(7):773-8.

Van Vlijmen OJ, Berge SJ, Swennen GR, Bronkhorst EM, Katsaros C, Kuijpers-Jagtman AM. Comparison of cephalometric radiographs obtained from cone-beam computed tomography\ scans and conventional radiographs. J Oral Maxillofac Surg 2009;67:92–97.

Walt B., and Jo Craven M. " Radiation Worries for Children in Dentists' Chairs" New York times (November 22, 2010)

VITA

NAME: Abdelrahman Ibrahim Salem

EDUCATION: D.D.S., University of Jordan, Amman, Jordan, 2009

M.S., Oral Sciences, University of Illinois at Chicago, Chicago, IL, 2014

Specialty Certificate, Orthodontics, University of Illinois at Chicago, Chicago, IL, 2014

HONORS: Honors Combined BS / DDS acceptance, University of Jordan, 2004

President's Honor Roll, University of Jordan, 2006-2009

Scholarship, University of Jordan, 2007

Summer Research Fellowship, University of Jordan, 2009

PROFESSIONAL: Teaching assistant, University of Jordan

MEMBERSHIP: American Association of Orthodontists (AAO)

American Dental Association (ADA)

Chicago Dental Society (CDS)

Illinois Society of Orthodontists (ISO)

Jordanian Dental Association (JDA)